Formation of dense branching morphology in the crystallization of Al-Ge amorphous thin films

Y. Lereah
Department of Electrical Engineering-Physical Electronics, Faculty of Engineering, Tel-Aviv University, Tel-Aviv 69978, Israel

G. Deutscher
Department of Condensed Matter Physics, School of Physics and Astronomy, Tel-Aviv University, Tel-Aviv 69978, Israel

E. Grünbaum
Department of Electrical Engineering-Physical Electronics, Faculty of Engineering, Tel-Aviv University, Tel-Aviv 69978, Israel

(Received 24 June 1991)

The crystallization of Al-Ge alloy amorphous thin films reveals a unique, dense branching morphology. Such morphology is found in other systems, i.e., electrodeposition and the Hele-Shaw cell, but so far this is the only known case in the field of materials science. A detailed description is given of the structure, morphology, and composition of the crystallized films and of the material processes that are involved in the crystallization of the Al-Ge alloy, and which are responsible for the unique morphology. The role played by diffusion is particularly emphasized.

PACS number(s): 64.60.−i, 61.16.Di, 68.35.Fx, 68.55.Jk

I. INTRODUCTION

The subject of "pattern formation" has been studied intensively during the last few years. This term is used to describe the morphology that is created during the front propagation of a phenomena and during the growth of a cluster, while subject to stable perturbations. One of the main motivations for these studies was the fractal dimensionality of the patterns, while another one was the universality of patterns that are created in different physical systems. The universality of the patterns can be best seen in a table published by Vicsek and Kertesz [1], in which three physical systems are presented: (a) two-dimensional electrodeposited clusters; (b) the viscous fingering in a Hele-Shaw cell; (c) the crystallization of liquids or amorphous materials. Each of these three systems exhibits similar morphologies, which are of three types: (i) the dentritic morphology, in which the anisotropy is a determining factor; (ii) the diffusion-limited aggregation (DLA) morphology, with a fractal dimension of 1.67; (iii) the dense branching morphology (DBM), with a dimension of 2.0, in which usually the influence of surface tension is observed.

The recently available large computation capability has been used to construct models for pattern formation in parallel to the laboratory experiments: The DLA morphology could be simulated, showing good similarity with experimental results [2], while by introducing different sticking coefficients, the influence of the surface tension, which represents noise reduction, could be demonstrated, and by introducing an anisotropic sticking coefficient, a dentritic morphology was simulated [3]. Recently it was shown that changing the diffusion length results in changing the object's dimension [4].

In the first two of the physical systems mentioned above the study is *ad hoc* and mainly concerned with geometrical aspects, while in the system of crystallization it forms part of phase-transition studies and has technological implications. The study in the latter system is concerned both with geometrical and thermodynamical aspects, the mechanism of the process and the microstructure of the material after crystallization. In this system only two of the morphologies mentioned above has been studied so far: The dentritic morphology has been known for a long time, but it is still the subject of many studies [5–7]. The DLA morphology is known only from very limited cases of crystallization of amorphous materials [8–10]. The formation of the dense branching morphology in materials science that enables intensive studies has been obtained for the first time in the present work of the crystallization of Al-Ge amorphous thin films [8,11,12].

The role played by stable perturbations in the formation of these morphologies was first given by Mullins and Sekerka [13], who studied liquid-solid phase transitions, giving rise to the dentritic morphology. They showed that if the planar front of a solid is propagating in the liquid under a field gradient (either of temperature in a pure substance or of concentration in a binary alloy) it will suffer from perturbations that are stable at a wavelength, that decreases with increasing propagation velocity of the growth front and with decreasing surface tension. The authors asserted that these stable perturbations are the origin of the dendrites often observed in crystals. For the growth of circular solids they found that the perturbation becomes stable when the diameter of the solid is seven times greater than that of the critical stable nucleus.

The crystallization of amorphous films has been intensively studied since the discovery of the amorphous metal glasses. In studies of the crystallization process, the amorphous films have the following advantages over liquids: (i) the process can be studied by *in situ* electron microscopy; (ii) the process can be stopped at intermediate stages for examination of the interface between the amorphous and crystalline phases, i.e., chemical analysis. In particular, the Al-Ge amorphous films have been found to be of interest for the following reasons: (iii) depending on the crystallization temperature, the growth of the crystalline phase can be as slow as a few angstroms per second; (iv) phase separation of Al and Ge is involved in the crystallization process; (v) the morphology of the crystalline phase is unique and can be modulated according to the crystallization temperature.

In previous studies of the slow crystallization of Al-Ge alloys the formation of colonies tens of micrometers in size was observed [14,15]. They contained small Al and Ge crystals. Koster [14] had pointed out the existence of an Al layer that surrounds these colonies through which Ge atoms diffuse for further growth. We had shown that this diffusion process leads to a branched morphology of the Ge core [12,16].

II. EXPERIMENTAL PROCEDURE

Thin films, 550 Å thick, of Al_xGe_{1-x} $(0.4<x<0.55)$ were prepared by simultaneous evaporation of Al and Ge from two electron-gun sources in vacuum of 10^{-6} torr. Two quartz thickness monitors were used, each placed in a pipe directed either toward the Al or the Ge sources. The evaporation rate of each element was about 4 Å/s. The substrates are microscope slides covered with smooth soluble material, held at room temperature. Due to geometrical considerations—the distance between the Al and Ge sources, the 75-mm length of the substrate, and the distance between the sources and the substrate—the concentration of the component varies along the slide up to a maximum of 10–15 % at the far edges. By cutting the glass into ten pieces, samples with differences of only 1–1.5 % could be obtained, each piece of glass supplied 10–20 identical samples of the thin films. The samples were mounted on 200–400 mesh grids of copper or nickel, the 400 mesh grid having the advantage of good thermal contact, while the 200 mesh grids have a large open area that is essential for EDS measurements.

The films were examined and heated in a transmission electron microscope (TEM) Philips EM300. A brief description of the TEM examination procedure, which is essential for the picture analysis, is given here. A high-voltage electron beam is transmitted through a thin film, and is partially diffracted as it passes areas that are in the proper Bragg condition. An aperture is placed in the back focal plan to let either the transmitted or a diffracted beam pass through it and to contribute to the bright- or dark-field pictures, respectively, which are formed by the electromagnetic lenses. The contrast in the bright-field picture arises as a consequence of differences in scattering for different materials (the higher the atomic number, the higher the scattering) and differences in the diffraction conditions. In the dark-field picture only the areas that diffract towards the aperture will be seen as bright, while the general field of view is dark.

The samples were heated during observation by using a commercial heating holder. The temperature is measured by a thermocouple that is placed in the furnace body. The measured temperature in the thermocouple differs from the temperature of area under observation as a result of heating this area by the electron beam, which is used for observation, on one hand, and as a result of finite-heat conduction by the grid and the film itself, on the other hand. Due to its small thickness, the film is buckled and is not in good contact with the grid everywhere; therefore, it is most useful to tilt the sample around an eucentric axis in the microscope in order to find a place in which the film and the grid are in the same plane, i.e., in good contact. The above sources of inaccuracies in temperature measurement, which are of opposite sense, give a total inaccuracy of 10 °C in measurements of the absolute temperature, but by working on the same open square of the grid under the same beam condition, the relative inaccuracy is only 1 °C (for further details see Ref. [17]).

The crystallization process was recorded by a sequence of photographs, each of them taken at an exposure time of a few seconds. Analysis of small areas, of about 1000 Å in diameter, were obtained by the x-ray energy dispersive spectroscopy technique (EDS) on partially crystallized films.

III. RESULTS AND DISCUSSION

A. The structure of the initial films

The as-prepared Al_xGe_{1-x} films, with x up to 0.55, were found to be amorphous, as is indicated by the broad halos in the electron-diffraction patterns. Films with higher Al concentration were found to be of granular structure, i.e., they contained small Al crystals embedded in an amorphous matrix. Here we will describe the crystallization of amorphous films; that of the granular films will be described elsewhere. Heating these films to temperatures of 230 °C or above results in their crystallization by nucleation and growth of colonies, which will be described in the following paragraphs.

B. The structure, morphology, and composition of the colonies

The colonies obtained by nucleation and growth during the crystallization of the amorphous Al-Ge films were nearly round, tens of micrometer in diameter. Such a colony is seen in Fig. 1. It consists of an Al-rich single-crystal matrix and a Ge polycrystalline core, composed of crystallites hundreds to thousands of angstroms in size.

The Ge core has a dense branching morphology (DBM). It is composed of branches, each starting with a certain minimal width, which increases during the branch's growth until it splits into two or three thin branches of the minimal width. Some of the branches stop growing, while those that keep growing come closer

to each other so that the core's dimension is two. The minimal width of the branches is probably determined by the Ge-Al surface tension, while the splitting is due to Mullins-Sekerka instabilities.

A dark-field image constructed by Ge diffraction spots shows that most of the Ge crystals are much smaller than the minimal branch width and a few of them are as large as the Ge branches (Fig. 2). The big Ge crystals tend also

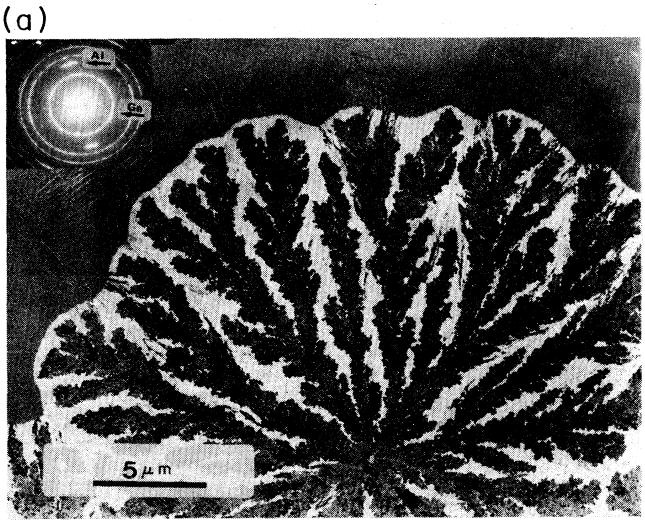

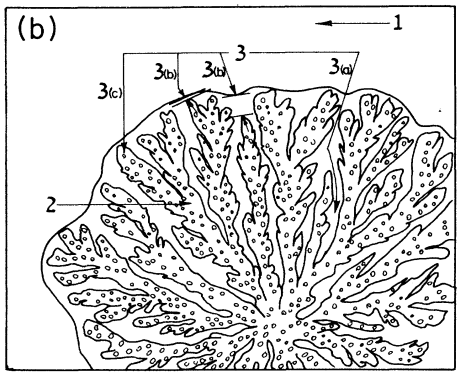

FIG. 1. (a) Electron micrograph of a typical Al-Ge colony surrounded by the amorphous phase. The dark core consists of polycrystalline Ge, which forms a dense branching morphology. The surrounding bright area is an (almost) single crystal of Al. It should be pointed out that the Ge is completely surrounded by Al; the dark regions that are seen to connect the Ge with the amorphous phase are actually rising from electron reflection in the Al crystal. The inset is an electron-diffraction pattern of the colony, indicating the microstructure of the components. (b) Schematic drawing explaining the microstructure and composition of the colony. Zone 1 is the amorphous phase in which the Al crystals grow. Zone 2 is the Ge core. Zone 3 is the Al single crystal in which the Ge core grows. 3(a) are the "fjords" between the Ge branches. 3(b) is the Al rim which separate the Ge core from the amorphous phase. 3(c) are small Al crystals embedded in the Ge core, they have the same crystallographic orientation as the Al crystal which surrounds the Ge core.

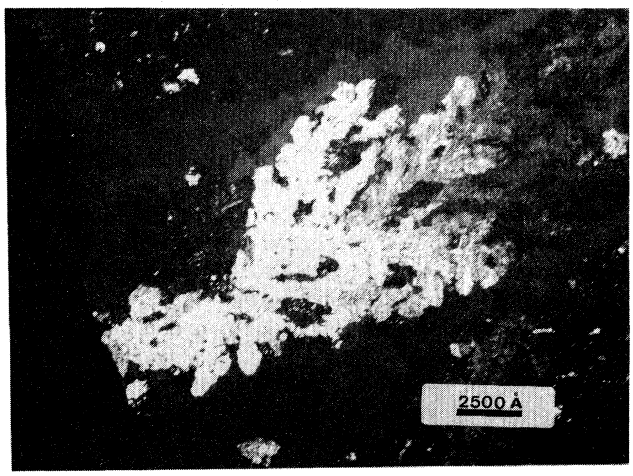

FIG. 2. A dark-field image created by a Ge diffracted beam. The core branches contain many small Ge crystals and a few large ones, which tend to broaden and to split.

to get broader and to split as they grow, but there is no one-to-one correlation between the Ge crystal and the branch splitting. It seems that the branches supply an envelope in which the Ge crystals nucleate and grow, while the larger Ge crystals are identical with the branch width.

The Al-rich single-crystal matrix completely surrounds the Ge core in the form of a rim and is also present in between the Ge branches, giving the impression of a "fjord-like" structure. Small disconnected Al crystallites are also present inside the Ge core. They have all the same orientation as the Al rim and fjords, as indicated by the fact that the electron-diffraction pattern of the complete colony (Fig. 1 inset) contains only Al arced spots. This is also confirmed by the dark-field image formed by an Al diffracted beam. It is clear that these crystallites stem from the same Al matrix. A high magnification micrograph of the boundary of the Al rim with the amorphous phase shows that it is very rough, at a scale of tens of angstroms (Fig. 3). It seems that the instabilities are of short range.

A quantitative analysis of the composition was obtained by the micro-x-ray energy dispersive analysis on spots of 1000-Å diameter in three different areas: (a) in the amorphous phase, at various distances from the colonies; (b) in the Al rim; (c) inside the Ge core. A schematic distribution of the Ge concentration is seen in Fig. 4.

(a) It was found that the Ge concentration is uniform in the amorphous phase, and is equal to the initial concentration (about 50%) even at spots touching the colony. This result is in disagreement with the classic model of crystallization from the liquid state, in which a concentration gradient is expected. It indicates that the Al diffusion length, if it exists at all, is very small, probably on a scale of tens to hundreds of angstroms, in agreement with the short range of Al front instabilities mentioned above.

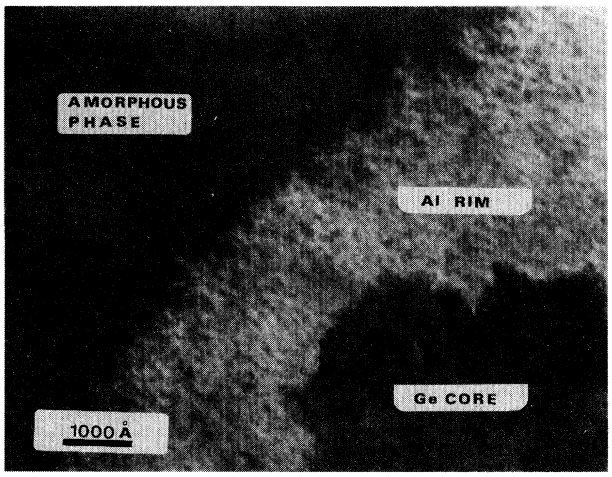

FIG. 3. The boundary between the Al and the amorphous phase at high magnification, showing the instabilities on the range of tens of angstroms.

(b) The Al rim was found to contain 9–12 at. % of Ge. As no isolated Ge crystals could be detected in the Al matrix by dark-field microscopy, it is concluded that the Ge is present in the Al as a solid solution. Such a concentration of Ge is much higher than that expected for the solid solution according to the equilibrium phase diagram. The high Ge concentration is explained by the extension of the solidus lines below the eutectic temperature [16]. Such an extrapolation is justified by two reasons: (i) the samples were initially quenched from the gas state, and during crystallization the temperature was not raised to the eutectic temperature, so that a steady state was never achieved, and (ii) the concentration deducted from this extrapolation is in agreement with the experimental results.

(c) The Ge core was found to contain on the average about 20 at. % Al; this value corresponds to the relative concentration of the small Al crystals that are present inside the Ge core [Fig. 1(b)].

The average Ge phase distribution as a function of the radial distance from the edge of the colony is plotted in Fig. 5. It represents the area-weighted average between the two phases present: the Al-rich matrix and the branched Ge core. The Al rim width (ξ) has been defined as the distance in which the core concentration decreases from 0.6 to 0.1.

No topographical features were detected on the film surface, except for some kind of dirt from inhomogeneities visible in the center of the colonies; they probably provide the nucleation sites.

C. The nucleation and growth of the colonies

The nucleation of the colonies occurs, mostly on the supporting grid and not in its open area. It is not clear if the metal contact is promoting the nucleation or if nucleation occurs on the supporting grid as a result of heat conduction considerations. As the nucleation of colonies is a rare event, it was impossible to "catch" a nucleation event under the field of view at high magnification. Such a study was obtained for films with higher Al concentration in which the nucleation rate is significantly in-

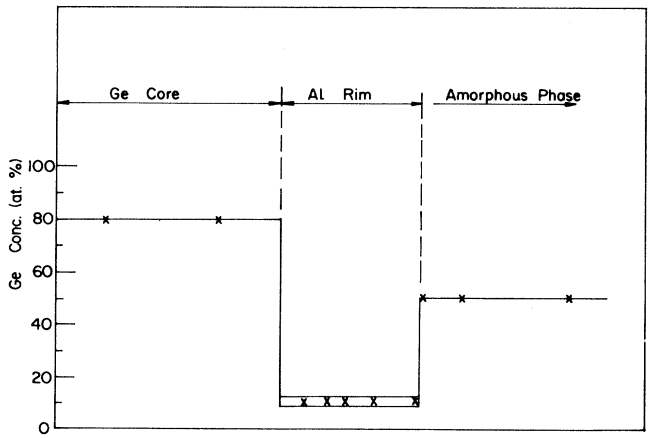

FIG. 4. A schematic distribution of the Ge concentration in different areas inside and outside of the colony.

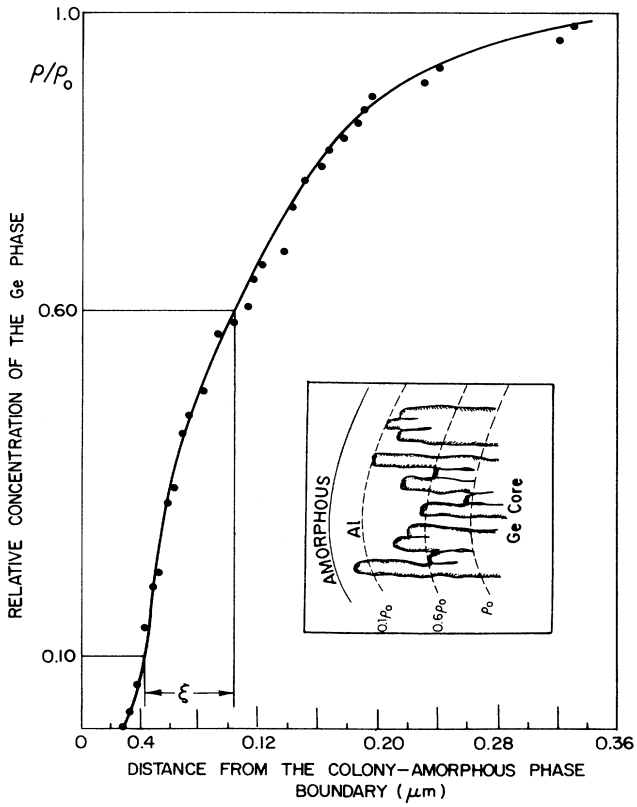

FIG. 5. Area weighted average Ge phase distribution as a function of the radial distance from the edge of the colony. The average rim width ξ is defined as the distance for which the average radial Ge phase distributions vary from 60% to 10%.

creased, and will be presented elsewhere. In the studies of the presented samples, the nucleation was observed under low magnification, so that the minimum colony size that could be detected is of 2–3 μm in diameter. On the other hand, these samples give good opportunity for the study of the growth process because once the colony nucleates, it grows a long distance.

Let us follow how such a colony grows. Figure 6 shows a colony at different stages of its growth. In Fig. 6(a) the colony is first detected at diameter of 3 μm. It contains a mixture of Ge and Al crystals, with no Al rim in its surrounding or branched cores. As the colony grows, the surrounding rim is developed [Fig. 6(b)] and increases up to a certain width [Fig. 6(c)], thereafter, the Al rim width remains constant. The Al rim width (ξ) as a function of the colony radius is seen in Fig. 7. The splitting of the Ge core starts when the Al rim reaches its maximum width [Fig. 6(c)].

The growth velocity of the colony is constant at a fixed temperature, independent of its radius (Fig. 8). The fluctuations in the velocity value around the average one, observed in Fig. 8, are probably due to the nucleation and growth events of the Ge crystals. Such an idea is supported by the interpretation of Raz, Lipson, and Polturak [18] of their measurements of the growth velocity fluctuations in ammonium chloride dentrites. The fluctuations of the velocity are more pronounced for small colonies in which the Ge big crystal size is comparable with the colony radius.

The processes involved in the colony growth are the following.

(*i*) *The growth of the Al single-crystal matrix in the amorphous phase.* This growth process has either no diffusion length or a very short one, as is indicated by the lack of gradient concentration in the Al stable front and by the short length scale roughness of its surface—tens to hundreds of angstroms.

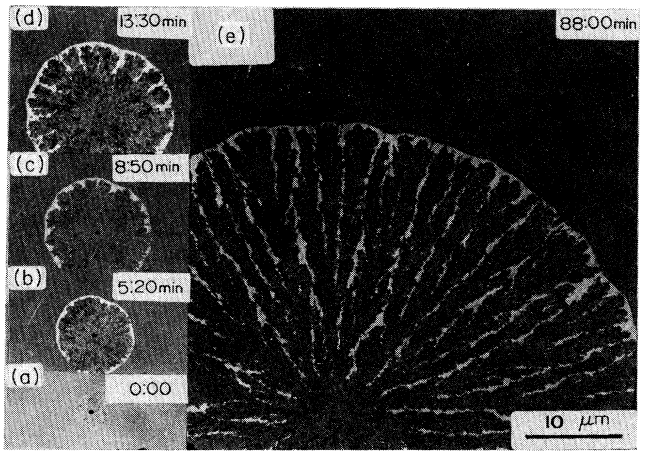

FIG. 6. The different stages in a colony growth. (a) shows the colony when it is first detected: it consists of a random mixture of Ge and Al crystals; no Al rim or Ge branched core is seen. A narrow Al rim can be seen in (b), whose width increases up to a certain value seen in (c); thereafter, the Al rim width is constant. The branching of the Ge core starts when the Al rim width reaches its maximum value [(c)].

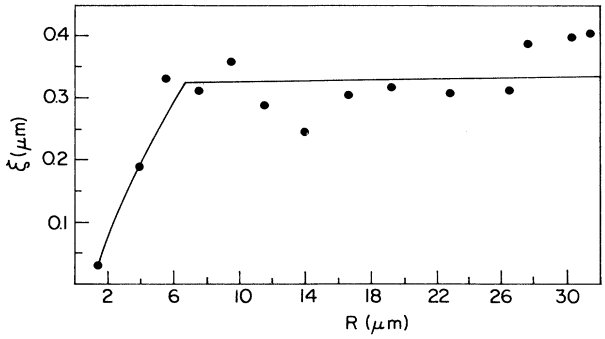

FIG. 7. Dependence of the Al rim widths on the colony radiuses. The splitting of the Ge core starts as the Al rim widths reaches its equilibrium value.

(*ii*) *The nucleation and growth of Ge crystals.* The nucleation of new Ge crystals occurs on the existing Al-Ge interface: no isolated Ge crystal was ever found. It seems that while the Al-Ge surface tension is low enough to enable the ramified structure of the Ge core, on one hand, it is not low enough to enable random nucleation of Ge crystals, on the other hand. These limitations of the Al-Ge interface are essential to the creation of the dense branching morphology of the Ge core inside the Al matrix.

(*iii*) *The diffusion of Ge through the Al rim.* As the Ge core is completely surrounded by the Al rim, its further growth depends on Ge atoms supplied from the amorphous Al-Ge phase. This Ge is supplied by diffusion through the Al rim, as can be concluded by the Laplacian morphology of the core. It was clearly seen that the Ge core growth occurs at the branch tips, which are nearest to the amorphous phase, i.e., where the continuous Al rim is narrowest.

The expected relation between the colony growth velocity (v), the Al rim width (ξ), and the diffusion coefficient of Ge in Al (D) is $v = D/\xi$. This relation was verified through temperature-dependent measurements, as will be seen in the next paragraph. It is interesting to note that the velocity (v) (Fig. 8) and the Al rim width ξ (Fig. 7) are constant during the colony growth, except for the very small colonies, in which the Al rim has not yet developed to its "mature" width. It shows how essential the creation of the branching morphology of the Ge core is for the continuous growth of the colony. If no splitting into branches occurred, the Al rim width would increase, as more and more Al would be rejected during the crystallization, and further growth of the colony would be slowed down, contrary to the observation. By its branched morphology, the Ge core can be locally kept at constant distance (ξ) from the amorphous phase—the source of the Ge atoms. It can be concluded that the reduction in the system's energy due to the crystallization is higher than the surface energy involved by the ramified morphology.

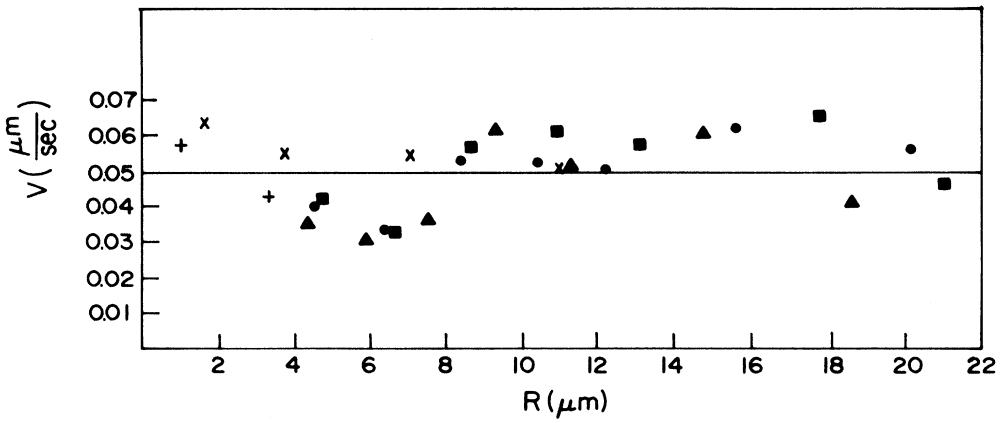

FIG. 8. The growth velocity v of the colony as a function of its radius R.

Crystallization of the Al-Ge amorphous films at 230–350 °C by slow-rate heating, using the furnace, reveal the colonies described in the previous sections whose growth velocity increased with crystallization temperature while their inner characteristic length scale decreased. Heating to higher temperatures and/or heating at a high rate by the electron beam reveal different morphologies, as well as the creation of unstable phases; neither issue will be described here. The growth velocity was found to increase exponentially from few angstroms per second at the low range of temperatures to few microns per second at the high range of temperatures (Fig. 9). From the slope of the graph, an activation energy of 3 eV was found for the colony growth process. The Al rim width (ξ) was found to decrease as the crystallization temperature increases. The relation D/ξ has also been plotted in this figure. D the diffusion coefficient at various temperatures, was taken from Ref. [19]. A comparison in Fig. 9 between the temperature dependence of the growth velocity and the relation D/ξ shows that they have the same slope and that the relation $v \propto D/\xi$ is indeed verified.

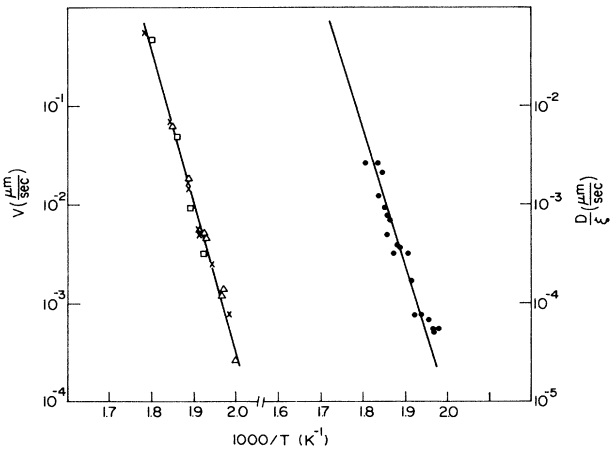

FIG. 9. A comparison between the dependence of colony growth velocity v and the ratio of D/ξ (D, diffusion coefficient of Ge in Al; ξ, the Al rim width) on temperature.

The Ge crystal size also decreases as the crystallization temperature increases, i.e., there are more Ge crystal nucleation events during the colony growth. This means that the Ge crystal nucleation rate increases with temperature faster than the total crystallization rate, i.e., the colony growth velocity; in other words assuming an exponential dependence of nucleation rate with temperature, the activation energy is higher. A quantitative measurement of the number of Ge crystals for a given area as a function of temperature [in order to find the nucleation rate ($\dot{N}$) dependence with temperature] is difficult to obtain because of the confusion in the dark-field image analysis of many bright spots either as small crystals or as a part of a bigger one which contains defects or strains. However, it was possible to obtain a comparative measurement of the number of Ge crystal for the extreme low and high crystallization temperatures. It was found that by increasing the colony growth velocity 250 times, the Ge crystal number in the same area increased by 7.5 times, which gives the relation $\dot{N}=v^{1.35}$. This result is in good agreement with the relation $v=(\dot{N}D)^{1/2}$, which replaces $v=\sqrt{BD}$ in the theory of Alexander *et al.* [16] by assuming that the reaction rate B is equal to the nucleation rate ($\dot{N}$) and by taking the relation $D=v^{1/2}$. This relation was found by comparing the dependence of v on temperature according to our finding and the dependence of D on temperature according to Ref. [19].

A comparison can be made between the formation of the dense branching morphology and the eutectic solidification. One of the unsolved questions in eutectic solidification is the mechanism of phase separation that takes place in the liquid in order to form the lamelar morphology. It seems that there exists a thin layer at the solid-liquid boundary in which the separation takes place [20]. In a liquid-solid transition, an observation of such a layer is impossible due to dynamical processes that occur at high temperatures. A procedure to study the eutectic process was developed, in which the samples are rapidly quenched after they are partially solidified. Using this procedure in a study of the Ge-Al alloy, Hellawell [21]

found that a thin Al layer exists between the solidified area and the liquid-quenched one. He had interpreted this thin layer as a consequence of the quenching process. The results of the present work on the crystallization of amorphous Al-Ge alloys suggest that this layer exists during the solidification and plays a role in the mechanism of phase separation. Similar results were found during the austenite-to-ferrite phase transition by Fisher and Darken in the 1960's. They found that when γ-Fe phase that is rich in carbon decomposes into α-Fe and Fe_3C, a Fe layer exists between the phases through which the C atoms diffuse to form lamelai of Fe_3C [22].

IV. SUMMARY

A unique morphology was created during the crystallization of amorphous Al-Ge films. The morphology is similar to the dense branching one, known from Hele-Shaw cell and electrodeposition systems. The main process that is responsible for this morphology is the diffusion of Ge atoms through the Al rim from the amorphous phase to the branched core in the crystalline phase. The splitting of the Ge core is essential for the continuous growth at constant velocity, as it creates a constant width of the Al diffusion barrier. The similarity of this morphology to the eutectic one is pointed out, suggesting the role that a thin layer can play in the phase separation.

ACKNOWLEDGMENTS

We thank S. Alexander, R. Bruinsma, and R. Hilfer for collaboration with the theory. We also thank E. Ben-Jacob and P. Garik for discussions on dense branching morphology and G. Thomas for discussion on the pearlite structure. This work was supported in part by the U.S.-Israel Binational Science Foundation and by the Oren Family Chair of Experimental Solid State Physics.

[1] T. Vicsek and J. Kertesz, Europhys. News **19**, 25 (1988).
[2] T. A. Witten and L. M. Sander, Phys. Rev. B **27**, 5686 (1983).
[3] J. Nittman and H. E. Stanley, Nature **321**, 663 (1986).
[4] R. L. Smith and S. D. Collins, Phys. Rev. A **39**, 5409 (1989).
[5] R. Trivedi and W. Kurz, Acta Metall. **34**, 1663 (1986).
[6] V. Laxmannan, J. Cryst. Growth **58**, 1652 (1987).
[7] A. Dougherty, P. D. Kaplan, and J. P. Gollub, Phys. Rev. Lett. **58**, 1652 (1987).
[8] Y. Lereah, in *Proceedings of the 43rd Annual Meeting of the Electron Microscopy Society of America, Louisville, 1985,* edited by G. W. Bailey (San Francisco Press, San Francisco, 1985), p. 346; G. Deutscher and Y. Lereah, Physica (Amsterdam) **140A**, 191 (1986).
[9] M. Ozenbas and H. Kalebozan, J. Cryst. Growth **78**, 523 (1986).
[10] Gy. Radnoczi, T. Vicsek, L. M. Sander, and D. Grier, Phys. Rev. A **35**, 4012 (1987).
[11] E. Ben-Jacob, G. Deutscher, P. Garik, N. D. Goldenfeld, and Y. Lereah, Phys. Rev. Lett. **57**, 1903 (1986).
[12] G. Deutscher and Y. Lereah, Phys. Rev. Lett. **60**, 1510 (1988).
[13] W. W. Mullins and R. F. Sekerka, Appl. Phys. **34**, 323 (1963).
[14] U. Köster, Acta Metall. **20**, 1361 (1972).
[15] M. J. Kaufman, J. E. Cunningham, Jr. and H. L. Fraser, Acta Metall. **35**, 1181 (1987).
[16] S. Alexander, R. Bruinsma, R. Hilfer, G. Deutscher, and Y. Lereah, Phys. Rev. Lett. **60**, 1514 (1988).
[17] Y. Lereah, G. Deutscher, and E. Grünbaum, in *Proceedings of the 11th International Congress on Electron Microscopy, Kyoto, Japan, 1986,* edited by T. Imura, S. Maruse, and T. Suzuki (The Japanese Society of Electron Microscopy, Tokyo, 1986), p. 323.
[18] E. Rax, S. G. Lipson, and E. Polturak (unpublished).
[19] N. L. Peterson and S. J Rothman, Phys. Rev. B **1**, 3264 (1970).
[20] L. M. Hogan, R. W. Kraft, and F. D. Lemeky, in *Advances in Materials Research,* edited by H. Herman (Wiley-Interscience New York, 1971), p. 83.
[21] A. Hellawell, Trans. Metall. Soc. AIME **239**, 1049 (1967).
[22] G. Thomas (private communication).

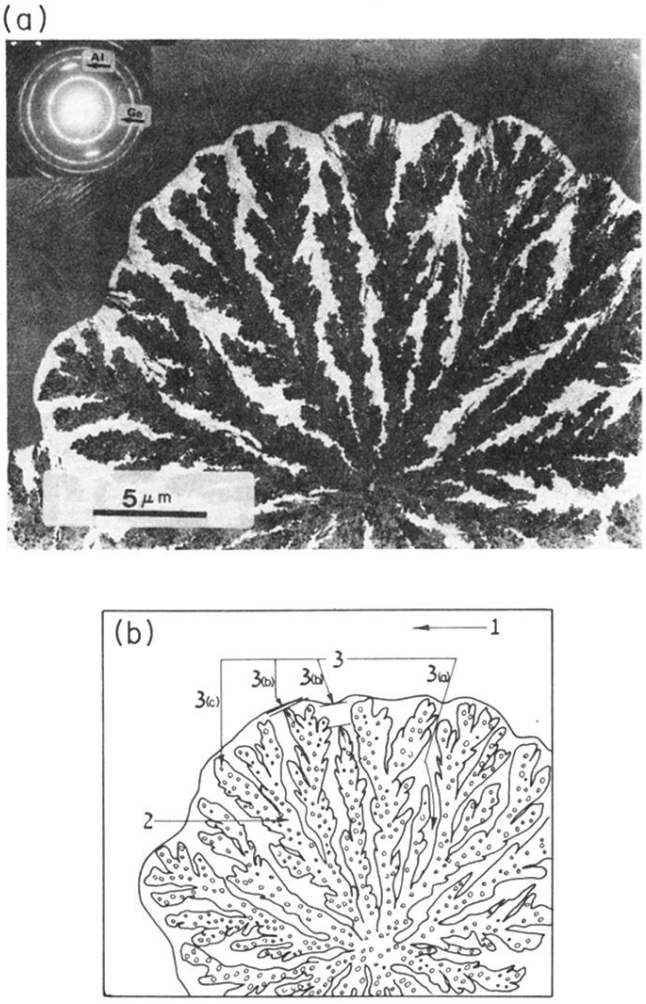

FIG. 1. (a) Electron micrograph of a typical Al-Ge colony surrounded by the amorphous phase. The dark core consists of polycrystalline Ge, which forms a dense branching morphology. The surrounding bright area is an (almost) single crystal of Al. It should be pointed out that the Ge is completely surrounded by Al; the dark regions that are seen to connect the Ge with the amorphous phase are actually rising from electron reflection in the Al crystal. The inset is an electron-diffraction pattern of the colony, indicating the microstructure of the components. (b) Schematic drawing explaining the microstructure and composition of the colony. Zone 1 is the amorphous phase in which the Al crystals grow. Zone 2 is the Ge core. Zone 3 is the Al single crystal in which the Ge core grows. 3(a) are the "fjords" between the Ge branches. 3(b) is the Al rim which separate the Ge core from the amorphous phase. 3(c) are small Al crystals embedded in the Ge core, they have the same crystallographic orientation as the Al crystal which surrounds the Ge core.

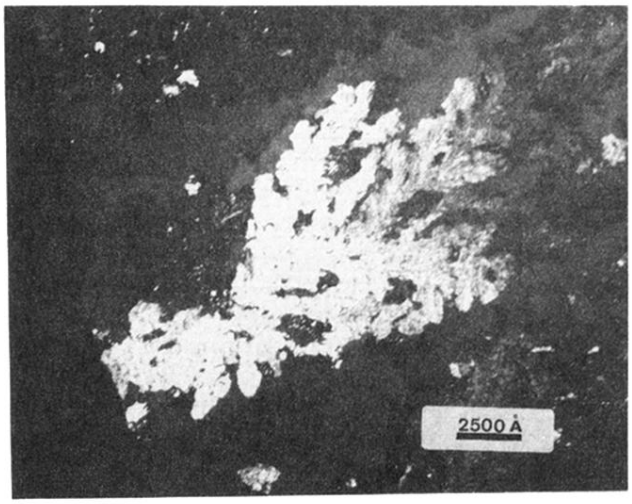

FIG. 2. A dark-field image created by a Ge diffracted beam. The core branches contain many small Ge crystals and a few large ones, which tend to broaden and to split.

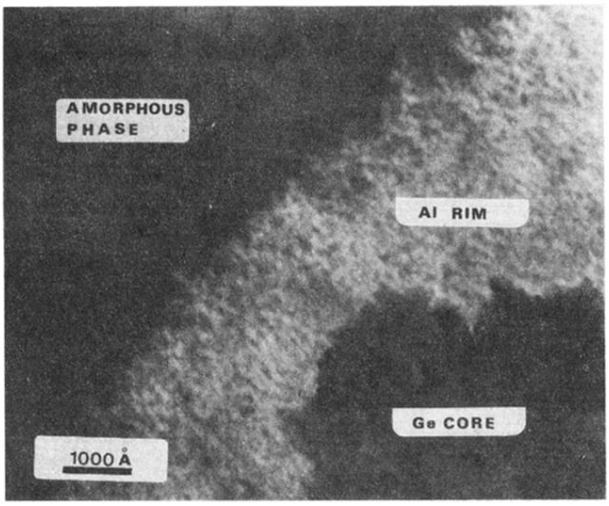

FIG. 3. The boundary between the Al and the amorphous phase at high magnification, showing the instabilities on the range of tens of angstroms.

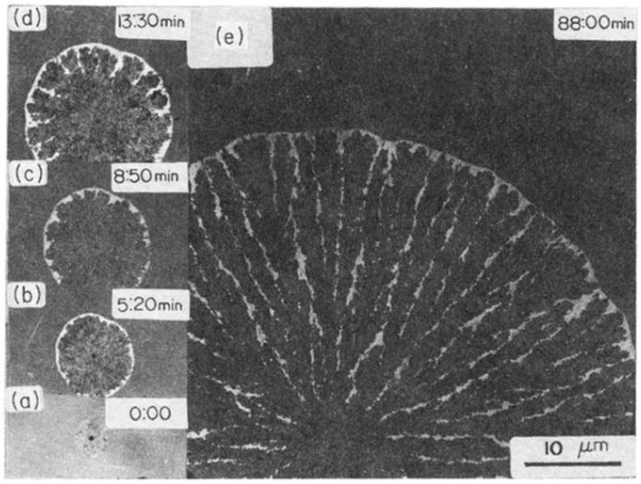

FIG. 6. The different stages in a colony growth. (a) shows the colony when it is first detected: it consists of a random mixture of Ge and Al crystals; no Al rim or Ge branched core is seen. A narrow Al rim can be seen in (b), whose width increases up to a certain value seen in (c); thereafter, the Al rim width is constant. The branching of the Ge core starts when the Al rim width reaches its maximum value [(c)].